SciMedCentral

Journal of Pharmacology & Clinical Toxicology

Research Article

Investigation of Structural Analogues of Azithromycin and Remdesivir for SARS-CoV-2 Mpro: A Computational Approach in Drug Development

Hridoy R. Bairagya[1]*, Sayanti Pal[1], and Sweety Gupta[2]

[1]*Department of Bioinformatics, Maulana Abul Kalam Azad University of Technology, India*

[2]*Department of Pharmaceutical Technology, Maulana Abul Kalam Azad University of Technology, India*

[#]*Authors (Sayanti Pal and Sweety Gupta) contributed equally to this manuscript and shared second authorship*

***Corresponding author**

Hridoy R. Bairagya, Computational Drug Design and Bio- molecular Simulation Lab, Department of Bioinformatics, Maulana Abul Kalam Azad University of Technology, West Bengal, India. Tel: 91-8277145815

Submitted: 14 July 2023

Accepted: 15 August 2023

Published: 18 August 2023

ISSN: 2333-7079

Keywords

- SARS-CoV-2 Mpro
- Two conformation
- Azithromycin
- Remdesivir
- Lopinavir Structural Analogues
- Molecular Docking.

Abstract

The Main protease (Mpro) is a vital enzyme of COVID-19 and plays an essential role, making it an attractive antiviral drug target. The antibiotic azithromycin was proven to be effective against influenza, remdesivir is a broad-spectrum antiviral agent that makes activity against various RNA viruses, and lopinavir is the peptidomimetic inhibitor of HIV protease that is recommended for COVID-19. The present computational study has introduced the virtual screening technique for drug repurposing and investigating the structural analogues for azithromycin, remdesivir, and lopinavir. Furthermore, molecular docking is used on active and inactive conformations in Mpro enzyme for comparative study of binding profile between azithromycin, remdesivir, and lopinavir and their analogs erythromycin, sofosbuvir and 3-Amino-N-{4-[2-(2,6-Dimethyl-Phenoxy)- Acetylamino]-3-Hydroxy-1-Isobutyl-5-Phenyl-Pentyl}-Benzamide respectively. The molecular docking between proposed drugs with the native conformation of Mpro demonstrates poor binding because the surface mouth region of the catalytic pocket of Mpro gets a closed form; thus, the drug could not reach the binding pocket. Hence, the findings on ligand-bound or active form signify the following vital information: (i) The antibiotic azithromycin may be used for COVID-19 disease because its structural analog erythromycin is loosely bound at the ligand-binding pocket. (ii) the antiviral remdesivir and its analog sofosbuvir have similar binding energy at the ligand-binding pocket of Mpro. Still, sofosbuvir has good drug score than remdesivir, and both may be used for COVID-19. (iii) lopinavir has poor binding energy at the active conformation of catalytic pocket rather than its analogue, and also, its drug score is worse than its analogue. We recommend that sofosbuvir is the best structural analogue for remdesivir and may further be considered to use in the preclinical study by replacing remdesivir, the analogues of lopinavir may be further synthesized and require proper experimental and preclinical investigation for the possible treatment of nCOVID-19. Our results were significant and evident in exploring our essential findings with the medical community.

ABBREVIATIONS

SARS-CoV-2: Severe Acute Respiratory Syndrome Coronavirus 2; COVID-19: Coronavirus disease 2019; WHO: World Health Organization; USAMRIID: U.S. Army Medical Research Institute of Infectious Diseases; GA: Genetic Algorithms

INTRODUCTION

The severe acute respiratory syndrome Coronavirus 2 (SARS-CoV-2) developed a historic number of illnesses and fatalities that has drastically impacted the daily routines life of people everywhere in world [1]. On March 11th, 2020, with the World Health Organization's (WHO) had declared a global pandemic situation for COVID-19 due to its tremendous societal and economic disruptions [2]. As per information from World Health Organization, there have been 767,518,723 confirmed cases for COVID-19 in internationally as of July 2nd, 2023 with involving 6,947,192 deaths. Although the limitation of human movement, such as travel bans, quarantines, containment, and mitigation technique are the option to prevent the COVID-19 [3]. Due to the high mortality rate for COVID-19, and despite the excellent efforts that have been applied, no approved drugs or some vaccines not been approved yet to combat the severity of the different mutant strains of SARS-CoV-2. Besides vaccine development, the recent demands an essential call for the discovery of new potential anti-COVID molecules. In this context, despite the use of recent medicine, natural products and their bioactive molecules executes adverse pharmacological and toxicological

properties [4]. Interestingly, macrolides remain an alternative option to consider the new drugs for COVID-19. Macrolides are a group of bacteriostatic antibiotics composed of 12 to 16 atoms lactone rings containing one or more deoxy sugars with usually attached cladinose and desosamine. The usefulness of macrolides is observed in broad spectrum with displaying activity of anti-inflammatory and antibacterial potency, commonly associated with respiratory tract infections in patients and viral pneumonia related to influenza and other viruses [5].

Azithromycin launched in 1991 has become one of the most widely used antimicrobials [6]. The azithromycin was proved to be effective against influenza complications of respiratory viral infections [7]. Recent studies have shown that patients treated with azithromycin in combination with hydroxychloroquine have been demonstrated to exhibit a virological cure for COVID-19 [8]. Azithromycin is described as an azalide that is structurally associated with the macrolide family of antibiotics. It is composed of fifteen- membered ring structure having two sugar moieties, several hydroxyl groups, two tertiary amino groups, and one oxycarbonyl group [9]. Clinical studies have demonstrated that patients suffering from both intermittent and chronic pseudomonas aeruginosa infection were treated using azithromycin [10,11]. Among other reasons, this antibiotic formulated mainly as suspension or tablets is used in human. Azithromycin may undergo multiple interactions with the analyte enantiomeric molecules [12], biological molecules and with the enzymes produce by COVID-19 for chiral recognition.

Remdesivir is a prodrug of adenosine triphosphate (ATP) analog, with potential antiviral or broad-spectrum antiviral agent activity against various RNA viruses [13]. Remdesivir (GS-5734) was developed by Gilead Sciences and emerged from collaboration between Gilead, the U.S. Centers for Disease Control and Prevention (CDC), and the U.S. Army Medical Research Institute of Infectious Diseases (USAMRIID) [14]. The major active metabolite of remdesivir is GS-441524, and its 1'-CN group and C-linked nucleobase ensure optimal anti-Ebola potency and selectivity against host polymerase enzymes. The remdesivir has demonstrated efficacy in both in vitro and in vivo models against Coronaviruses. Based on these clinical findings, the U.S. Food and Drug Administration have issued an Emergency Use Authorization of the use of remdesivir to treathospitalized COVID-19 patients [15]. With no drug having FDA approval for marketing as a treatment for SARS-CoV-2, this is the first FDA authorization of an investigational therapeutic for use in treating SARS-CoV-2.

Lopinavir is one of the peptidomimetic inhibitor of HIV protease which binds to the catalytic site of the HIV protease. It was first approved in 2000 in the United States as the therapeutics of HIV infaection both in adult as well as children, lopinavir is generally administered in combination with Ritonavir to improve the metabolism of lopinavir in the treatment of HIV infection [16]. During the early phases of the pandemic, lopinavir/ritonavir was recommended for treatment purposes of COVID-19 but is presently not indicated for the same in both hospitalized and outpatient patients [17]. A recent study highlighted that large randomized clinical investigations must be performed to assess lopinavir/ritonavir combined with interferon to treat COVID-19 [17,18].

The Main protease (Mpro) of SARS-CoV-2 is a crucial enzyme of Coronaviruses and has a pivotal role in mediating viral replication and transcription and making it as an attractive drug target for SARS-CoV-2 [19]. The monomer of Mpro is enzymatically less active. At the same time, the most hydrolytic activity is seen in its dimeric form, which serves as a functional unit with two 306-residue long [20]. The Mpro contains three domains, domain I (residues 8–101) and domain II (residues 102–184) have an antiparallel β-barrel structure. Domain III (residues 201–303) contains five α-helices arranged into a largely antiparallel globular cluster, and it is connected to domain II by a long loop region (residues 185–200). A catalytic dyad transfers a single proton from Cys145 to His41. At the same time, Cys145's sulfur atom engages in a nucleophilic attack on the carbonyl carbon of the peptide bond to produce an intermediate known as thiohemiketal. The zwitter catalytic dyad Cys–145–His^{+}41 needs to be activated by energetically water that is maintained by His164 and Asp18.

Multiple analyses of crystal structures of the native and ligand-bound state of Mpro protein provide suggestions into which conformation will be considered for further investigation. Thus, this is the first computational report that explores molecular docking results on the two alternative conformations of catalytic His41 of the Mpro enzyme. In the native state, the geometrical orientation of the ND1 atom in His41 and its NE2 of ligand-bound form is facing toward the surface of the catalytic pocket and may interact with the proposed ligand. For this, molecular docking was performed to screen the structural analogues of azithromycin, remdesivir and lopinavir drug against two conformations of SARS-CoV-2-Mpro receptors to investigate the potential inhibitors of its catalytic domain. These findings may be beneficial for controlling the propagation of the Novel Coronavirus (COVID-19) as well as the prediction of a new medication. No computational study has yet been reported on structural analogues of azithromycin, remdesivir and lopinavir with two new conformations of Mpro protein to capture the conformational transitions. Our computational techniques act as a complementary approach for repurposing of drugs. The vision of present study is to evaluate the inhibitors that are structurally similar to of azithromycin, remdesivir and lopinavir.

MATERIALS AND METHODS

Structure collection

The crystal structures of the dimers of SARS-CoV-2 Main Protease (Mpro) were obtained from the RCSB Protein Databank [21] to choose molecular docking receptors. On the basis of structural information, the two criteria were adopted for receptor selection; (i) native and (ii) ligand-bound conformation. The PDB Id. 7NTT (resolution 1.74Å) is the native form where

ND1 of His41 faces towards the surface of ligand binding pocket. In contrast, the PDB Id. 7VLP (resolution 1.50Å) is the ligand-bound form and its NE2 of His41 adopts the open face. Therefore, the ND1 and NE2 atoms of His41 were considered as the center point for molecular docking investigation.

Identification of Mpro pockets

The pockets of Mpro proteins (native and ligand-bound form) were identified using the program Computed Atlas of Surface Topography of Proteins (CASTp) [22], to find out atoms of residues that constitute the active site surface for the catalytic region. The functionality of CASTp, for measuring protein pockets and cavities, is based on accurate computational geometry methods with solvent probe sphere 1.40 Å.

Investigation of structural analogs for Virtual screening and QSAR property analysis

The SMILES of azithromycin (DB00207), remdesivir (DB14761), and lopinavir (DB01601) were obtained from the Drug-Bank database (v5.1.5) [23], and it was used for high throughput screening to investigate structural analogs of these drugs by Swiss Similarity program (Figure 1) [24]. One library (drug bank) was chosen for the high throughput screening (HTS) to achieve the best structural analogues of azithromycin, remdesivir, and lopinavir. After HTS, the ~400 structural analogues from azithromycin, remdesivir, and lopinavir drugs are observed with reasonably good similarity scores, and finally, the best three azithromycin analogues: erythromycin, clarithromycin, and dirithromycin (similarity score 0.95), one remdesivir analogue sofosbuvir (with similarity score 0.46), and three lopinavir analogues (similarity score 0.66) were obtained from DrugBank on the basis of SWISS similarity score (Figure 2) for further molecular docking study with 7NTT and 7VLP crystal structure.

The Osiris property explorer [25], and Swiss-ADME [26] programs have been used to compare the pharmacokinetics and drug-likeness scores between azithromycin, remdisivir, and lopinavir and their analogues. Each molecule was filtered out based on six molecular properties (cLogP, solubility, molecular weight, TPSA, drug-likeness, and drug score) from the Osiris program and four characters (molar refractivity, Lipinski, bioavailability score, and synthetic accessibility) from Swiss-ADME program.

Molecular Docking Study Receptor and Ligand Preparation

Two conformations of receptor molecules and six ligands were prepared using AutoDockTools (ADT, v1.5.6) [27]. The native (PDB Id. 7NTT) and ligand-bound (PDB Id. 7VLP) protein structures were taken as the receptor for the molecular docking study. Then ligands, water molecules, and heteroatoms were removed from two crystal structures, polar hydrogen bonds and Gasteiger charges were added, respectively, and the structures were prepared in pdbqt format. The six ligands azithromycin (DB00207), erythromycin (DB00199), remdesivir (DB14761), sofosbuvir (DB08934), lopinavir (DB01601), 3-Amino-N-{4-[2-(2,6-Dimethyl-Phenoxy)-Acetylamino]-3-Hydroxy-1- Isobutyl-5-Phenyl-Pentyl}-Benzamide (DB04378) were obtained from DrugBank. The Kollman-united charge was used to calculate the partial atomic charge of each ligand, and their torsional angles with rotatable bonds are assigned, and the files are saved in PDBQT format. The rotatable bonds of azithromycin,

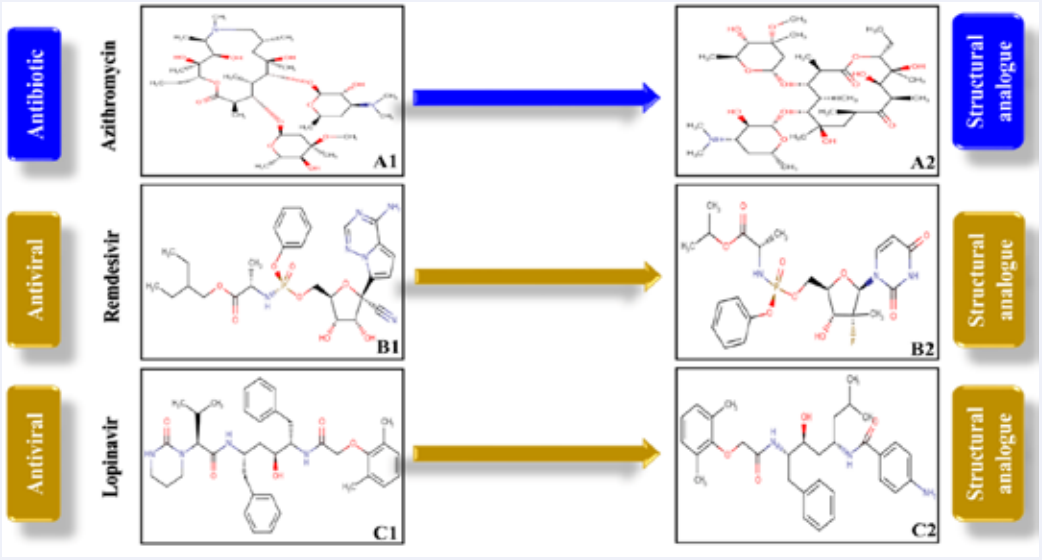

Figure 1 2-Dimensional (2D) structures of the proposed Anti-Covid Drugs; (A1) 2D structure of azithromycin; (A2) 2D structure of structural analogue of the azithromycin; (B1) 2D structure of remdesivir. (B2) 2D structure of structural analogue of the remdesivir; (C1) 2D structure of lopinavir; (C2) 2D structure of structural analogue of the lopinavir.

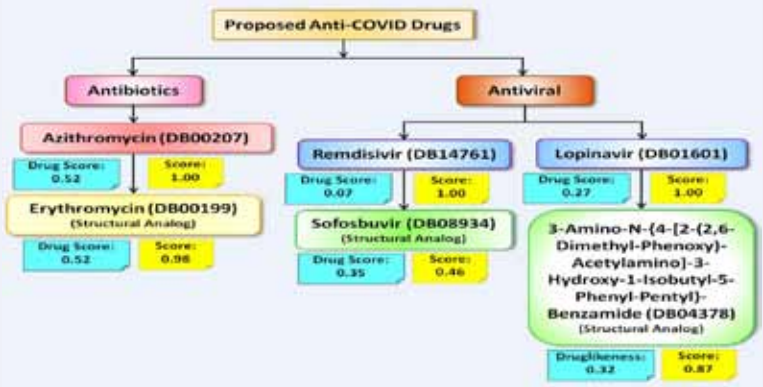

Figure 2 Schematic representation of Proposed Anti-COVID Drugs.

erythromycin, remdesivir, sofosbuvir, lopinavir, 3-Amino-N-{4-[2-(2,6-Dimethyl-Phenoxy)-Acetylamino]-3 Hydroxy-1- Isobutyl-5-Phenyl-Pentyl} Benzamide are four, two, twelve, ten, eight, and six respectively.

Molecular Docking

The molecular docking was employed using AutoDockTools 1.5.7 [27], and Autodock 4.0 program [28], for grid generation and docking, respectively. The conformations of two receptors, 7NTT and 7VLP, were kept fixed (rigid), and all the ligands were prepared as flexible with appropriate assigning their rotatable bonds. The docking was performed using the following protocols: category-I assigning ND1 of His41 as coordinates of the central grid point and category-II in NE2 of His41. In the grid box for category-I and II dockings, the size of the cubic grid box was defined as 60×60×60 Å. Affinity maps for all the present atom types and an electrostatic map were computed with a grid spacing of 0.375 Å. The number of Genetic Algorithms (GA) [29], runs performed for the docking was 100 runs, and each run was ranked based on its binding energy. The structural models were collected from the lowest-energy docking solution of each cluster of AutoDock. The docked ligand–protein complexes were visualized on Pymol 2.5.5 [30], for image construction. The binding energies and affinities for the ligands were obtained from the log files of the docks generated by AutoDock.

RESULTS AND DISCUSSION

Analysis of ligand-binding pocket in Mpro-crystal structures

The nine crystal structures of native and twenty-one of ligand-bound dimeric conformations of Mpro proteins were obtained from the Protein Data Bank. Several research groups have independently solved these structures using PHENIX, REFMAC, BUSTER, or nCNS refinement programs at 4.6–8.5 pH. The crystallographic structural parameters (c.s.p.) such as Matthews coefficient, solvent content, and calculated mean B- factors of protein are found maximum in 7VK3 and 7VK4 of native and 7VLQ in ligand- bound conformation. Moreover, the observed ratio of the number of protein atoms concerning water molecules (NPROT/NHOH) in Mpro-native and ligand-bound form are different ranges that suggest 7VK7 of native and 7NT1 of the ligand-bound ensemble are actually random compared to remaining structures (Table S1 and S2). Therefore, 7NTT of native and 7VLP of ligand-bound form were considered as reference structure for the present computational study.

The catalytic pocket of the native inactive conformation of Mpro is organized in such a way so that the NE2 and ND1 of the imidazole group of His41 are packed with Cys145 and one catalytic water molecule, respectively. The ND1 of His41 is also facing toward the surface of the pocket. In contrast, the NE2 and ND1 of His41 in ligand-bound active conformation make H-bond with ligand and Cys145. Moreover, its NE2 position also occupies at the front of surface. The superimposed complex structure between native and ligand-bound form has clearly shown the imidazole group of His41 rotates (dihedral angle of Chi 2) ~2^0, and the ND1 position of His41 is reversely orientated from front area of catalytic pocket to its backside during the conformational transition from native to ligand-bound form (Figure 3). Therefore, two alternative conformations of Mpro are considered as receptors for the present investigation to pay attention to the binding mode of each drug at the concern pockets for comparative study. The CASTp analysis reveals the volume of catalytic pocket of native and ligand-bound structure are ~ 444.30 and 560.70 $Å^3$ respectively (Table S3 and S4) that demonstrate the volume of the concern pocket are large in ligand-bound state compare to inactive monomer Mpro. Thus, we will examine how the proposed drug tightly and stereo-chemically binds at the catalytic pocket in the inactive native and active ligand-bound conformation. This investigation will definitely reveal the new insight about the drug (antibiotic or antiviral)-receptors interactions for repurpose the existing drug for COVID-19.

Binding mode prediction of azithromycin, remdesivir, lopinavir and their structural analogues and analysis of their pharmacological properties

The computational molecular docking studies are effective

SL. NO.	PDB Id	RESOLUTION (Å)	R-VALUE FREE/ R VALUE WORK	SPACE GROUP	CHAINS/ SEQUENCE LENGTH	REFINEMENT METHOD	UNIT CELL		CRYSTALLOGRAPHIC PARAMETERS					NO. OF REFLECTIONS
							LENGTH (Å)	ANGLE (°)	PH	SOLVENT CONTENT	MATHEWS COEFFICIENT	MEAN ISOTROPIC B FACTOR	RATIO (protein/ water)	
01	7MTT	1.74	0.26/0.21	P 1 21 1	A/B/306	REFMAC	a=44.76 b=53.91 c=114.35	α= 90 β=101.13 γ= 90	NIL	38.6	2	29.06	17.66	52472
02	7VPW	2.20	0.28/0.22	P 21 21 21	A/B/306	PHENIX	a=69.1 b=104.1 c=105.5	α= 90 β= 90 γ= 90	8.5	56.98	2.86	56.68	73.68	39287
03	7VJX	2.20	0.25/0.26	P 21 21 21	A/B/306	PHENIX	a= 69.2 b=104.3 c=105.7	α= 90 β=90 γ= 90	8.5	57.21	2.87	62.04	47.86	39396
04	7VE9	2.10	0.24/0.24	P 21 21 21	A/B/306	PHENIX	a= 69.2 b=104.3 c=105.7	α= 90 β= 90 γ= 90	8.5	57.21	2.87	58.49	44.63	45326
05	7VE3	2.10	0.28/0.24	P 21 21 21	A/B/306	PHENIX	a= 69.3 b=104.4 c=105.7	α= 90 β= 90 γ= 90	8.5	57.31	2.88	53.55	40.72	42380
06	7VE4	2.10	0.27/0.23	P 21 21 21	A/B/306	PHENIX	a= 68.9 b=103.9 c=105.2	α= 90 β=90 γ= 90	8.5	56.86	2.85	64.73	659.71	44742
07	7VE5	2.17	0.27/0.24	P 21 21 21	A/B/306	PHENIX	a= 69.2 b=104.3 c=105.6	α= 90 β= 90 γ= 90	8.5	57.17	2.87	57.49	58.76	41092
08	7VE6	2.25	0.27/0.24	P 21 21 21	A/B/306	PHENIX	a= 104.8 b=105.5 c=69.1	α= 90 β=90 γ= 90	8.5	57.66	2.86	60.86	45.07	36760
09	7VE7	2.40	0.24/0.21	P 21 21 21	A/B/306	PHENIX	a= 69.1 b=104.3 c=105.5	α= 90 β= 90 γ= 90	8.5	57.66	2.86	77.57	76.10	30465

Table S1 Schematic representation of Proposed Anti-COVID Drugs.

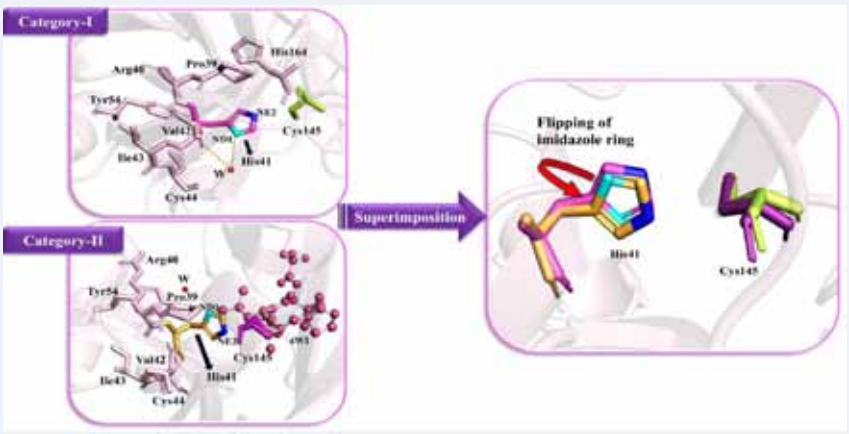

Figure 3 Superimposed complex structure between native (Category-I) and ligand-bound (Category-II) showing the imidazole group of His41 rotates (dihedral angle of Chi 2) ~20, and the ND1 position of His41 is reversely orientated from front area of catalytic pocket to its backside during the conformational transition from native to ligand- bound conformation.

Table S2: Crystallographic details of the dimers of Ligand-bound Mpro

Sl. No.	Pdb Id	Resolution (Å)	R-Value Free/ R Value Work	Space Group	Chains/ Sequence Length	Refinement Method	Unit Cell		Crystallographic Parameters					No. Of Reflections
							Length (Å)	Angle (°)	Ph	Solvent Content	Mathews Coefficient	Mean Isotropic B Factor	Ratio (Protein/ Water)	
01	6Y2G	2.20	0.25/ 0.19	P 21 21 21	A/B/306	REFMAC	a = 68.57 b =101.60 c =103.70	α = 90 β = 90 γ = 90	8.5	53.92	2.67	40.89	14.92	37448
02	7DGG	2.00	0.22/0.18	P 1 21 1	A/B/306	PHENIX	a = 55.80 b =99.12 c =59.75	α = 90 β=108.99 γ = 90	6	46.75	2.31	26.85	13.35	37990
03	7DGI	1.90	0.21/0.18	C 2 2 2 1	A/B/306	PHENIX	a = 64.67 b =118.20 c =223.27	α = 90 β = 90 γ = 90	6	61	3.15	26.66	7.28	67801
04	7DK1	1.90	0.21/0.19	P 21 21 21	A/B/306	BUSTER	a = 67.62 b =102.2 c =102.35	α = 90 β = 90 γ = 90	6.5	53.4	2.64	39.17	10.78	56431
05	7DPU	1.75	0.20/0.17	P 1 21 1	A/B/306	PHENIX	a = 44.26 b =53.80 c =115.06	α = 90 β=100.96 γ = 90	NIL	38.13	1.99	23.83	11.35	52603
06	7EN8	1.83	0.27/0.23	P 21 21 21	A/B/306	PHENIX	a = 54.83 b =67.86 c =167.56	α = 90 β = 90 γ = 90	4.6	46.61	2.3	15.61	8.67	55655
07	7FAZ	2.10	0.24/0.19	P 21 21 21	A/B/306	PHENIX	a = 67.61 b =97.96 c =101.59	α = 90 β = 90 γ = 90	NIL	50.53	2.49	40.63	12.05	39929
08	7NT1	2.85	0.28/0.20	P 21 21 21	A/B/306	REFMAC	a =68.18 b =102.17 c =104.38	α = 90 β =90 γ = 90	6.5	54.29	2.69	56.79	87.13	17333
09	7NT2	2.15	0.25/0.20	P 21 21 21	A/B/306	REFMAC	a = 68.16 b =100.59 c =104.73	α = 90 β = 90 γ = 90	6.5	53.71	2.66	40.00	26.15	39220
10	7NT3	2.33	0.27/0.21	P 21 21 21	A/B/306	REFMAC	a = 68.01 b =101.35 c =103.98	α = 90 β = 90 γ = 90	6.5	53.63	2.65	49.32	37.23	31556
11	7NW2	2.10	0.22/0.19	P 21 21 21	A/B/306	BUSTER	a = 67.45 b =99.75 c =103.61	α = 90 β = 90 γ = 90	6.5	52.25	2.58	36.83	13.01	39471
12	7TLL	1.63	0.25/0.21	P 1 21 1	A/B/306	BUSTER	a = 45.39 b =53.82 c =115.54	α = 90 β=102.42 γ = 90	NIL	39.54	2.03	27.23	14.21	53153
13	7U28	1.68	0.25/0.21	P 1 21 1	A/B/306	BUSTER	a = 45.55 b =53.80 c =114.89	α = 90 β=102.13 γ = 90	NIL	39.48	2.03	23.93	14.86	46261
14	7U29	2.09	0.27/0.20	P 1 21 1	A/B/306	BUSTER	a = 45.52 b =55.79 c =114.23	α = 90 β=105.22 γ = 90	NIL	40.49	2.07	30.31	23.58	28383
15	7VLP	1.50	0.22/0.20	P 1 21 1	A/B/305	PHENIX	a = 55.48 b =98.70 c =59.42	α = 90 β=108.72 γ = 90	NIL	45.85	2.27	23.30	18.62	94010
16	7VLQ	1.94	0.23/0.20	P 21 21 21	A/B/300	PHENIX	a = 67.85 b =102.02 c =103.27	α = 90 β =90 γ = 90	NIL	54.56	2.71	26.58	22.27	51406
17	7VTH	2.00	0.26/0.21	P 1 21 1	A/B/311	REFMAC	a = 44.41 b =54.27 c =114.50	α = 90 β =99.42 γ = 90	NIL	37.79	1.98	18.55	20.34	34366
18	7VU6	1.80	0.28/ 0.22	P 1 21 1	A/B/308	REFMAC	a = 55.47 b = 99.23 c = 58.88	α = 90 β=108.05 γ = 90	NIL	45.76	2.27	17.80	12.88	52687
19	7VVT	2.51	0.25/0.23	P 21 21 21	A/B/306	PHENIX	a = 67.99 b =30.12 c =103.18	α = 90 β =90 γ = 90	NIL	47.35	2.34	50.70	77.75	22010
20	7WYP	2.30	0.27/0.22	P 21 21 21	A/B/306	PHENIX	a = 67.81 b =101.28 c =103.15	α = 90 β = 90 γ = 90	7.5	53.01	2.62	55.30	57.09	32303
21	7XAR	1.60	0.21/0.17	P 1 21 1	A/B/306	REFMAC	a = 47.03 b =63.36 c =102.83	α = 90 β = 90.40 γ = 90	NIL	45.68	2.26	22.40	10.01	76114

Table S3: Identification of Pockets in dimer Native-Mpro (PDB Id: 7NTT)

Sl. No.	MS Volume (Å^3)	Pocket MS Area (Å^2)	Openings	Mouth MS Area (Å^2)	Sequence
1	2195.5	1170.1	4	295.4	Ser1, Gly2, Phe3, Arg4, Lys5, Arg131, Lys137, Gly138, Thr169, Gly170, Val171, Thr199, Trp207, Asn214, Asp216, Leu282, Gly283, Ser284, Ala285, Leu286, Leu287, Glu288, Asp289, Glu290, Phe291
2	803.9	339.4	1	325.4	Tyr237, Asn238, Tyr239, Leu271, Leu272, Gly275, Met276, Asn277, Gly278, Ala285, Leu286, Leu287
3	1215.1	753.7	3	252.3	Pro9, Gly11, Lys12, Glu14, Gly15, Met17, Trp31, Ala70, Gly71, Lys97, Pro122, Phe305, Gln306
4	444.3	272.2	1	107.7	Thr24, Thr25, Thr26, Leu27, His41, Cys44, Ser46, Met49, Phe140, Leu141, Asn142, Gly143, Ser144, Cys145, His163, His164, Met165, Glu166, Gln189
5	314	205.7	1	115.3	Gln107, Pro108, Gly109, Gln110, Pro132, Ile200, Val202, Asn203, Glu240, Asp245, His246, Ile249, Thr292, Pro293, Phe294
6	127	77.9	1	68.5	Leu220, Asn221, Arg222, Gly258, Ile259, Asp263

Table S4: Identification of Pockets in dimer Ligand-bound Mpro (PDB Id: 7VLP)

Sl. No.	MS Volume (Å^3)	Pocket MS Area (Å^2)	Openings	Mouth MS Area (Å^2)	Sequence
1	2240.00	1218.10	5	392.50	Gly2, Phe3, Arg4, Lys5, Arg131, Lys137, Gly138, Ser139, Phe140, Leu141, Glu166, Thr169, Gly170, Val171, His172, Trp207, Asn214, Leu282, Gly283, Ser284, Leu286, Glu288, Asp289, Glu290, Phe291, Gln299, Cys300
2	665.50	333.40	2	232.60	Gly11, Lys12, Glu14, Gly15, Lys97, Asp155, Thr304
3	560.70	292.10	1	135.50	Thr25, Thr26, Leu27, His41, Met49, Phe140, Leu141, Asn142, Gly143, Ser144, Cys145, His163, His164, Met165, Glu166, Asp187, Arg188, Gln189
4	155.70	97.50	1	111.10	Glu14, Gly71, Ser121, Pro122
5	198.10	189.30	1	16.10	Ser123

tools, which are broadly utilized to interpret the molecular aspects of ligand–protein interactions during drug discovery against various prior fatal and emerging diseases including SARS coronavirus. Our computational drug repurposing workflow against Mpro-native and ligand-bound were started with a docking of five FDA-approved drugs and one new ligand using AutoDock program. In this approach, we elucidate how the ligands are occupying in the binding site of native and ligand-bound state. To do so, we exhaustively searched the proper and accurate orientation of each docked ligand, so that corresponding atoms of the respective ligand can occupy the positions at His41's ND1 in native form (Figure 4) or NE2 in ligand-bound form (Figure 5).

Analysis of molecular docking results showed the anti-biotic azithromycin binds with Gln189 and Thr26 in the native state (binding energy -4.52 kcal/mol) and Cys145, Gln189, and Ser46 in ligand-bound state (binding energy -8.83 kcal/mol) (Figure 6 and Table 1). Moreover, its analog erythromycin makes H-bond with Ser46 and His41 in native form (binding energy -6.93 kcal/mol) and Gln166 and Asn142 in ligand-bound form with binding energy (-7.26 kcal/mol) (Figure 7). Furthermore, the anti-viral remdesivir makes complex with Thr24, Thr25, Thr26, Asn142, and Gly143 in native Mpro (binding energy-7.37 kcal/mol) and Cys45, Ser144, His163, Glu166 and Arg188 in ligand-bound form (binding energy-8.94 kcal/mol) (Figure 8). However, its analogue sofosbuvir binds at the catalytic pocket with Thr26, Ser46, and Gln189 in native form (binding energy -7.62 kcal/mol) and His41, Thr26, His164 in ligand-bound form (-8.94 kcal/mol) (Figure 9). Moreover, lopinavir makes H-bond with Thr24, His164, and Asn142 in native structure (binding energy -7.64 kcal/mol) and -5.50 kcal/mol in ligand- bound structure (Figure 10). In addition, its analogue: 3-Amino-N-{4-[2-(2,6-Dimethyl-Phenoxy)-Acetylamino]-3-Hydroxy-1-Isobutyl-5-Phenyl-Pentyl}-Benzamide also make interaction with Ser46 and Glu166 (binding energy -4.35 kcal/mol) and His41, Asp187, and Tyr54 in ligand-bound state (binding energy -8.58 kcal/mol) (Figure 11). The superimposed complex structures between docked and the reference ligand (4WI) of crystal structures suggest all the docked ligands occupy near the position of reference ligand (Figure 12). Consequently, the structural analog sofosbuvir, 3-Amino-N-{4-[2-(2,6-Dimethyl-Phenoxy)-Acetylamino]-3-Hydroxy-1-Isobutyl-5-Phenyl-Pentyl}- Benzamide and remdesivir bind regeo-specially at NE2 position of His41 in the ligand- bound Mpro (Figure 13).

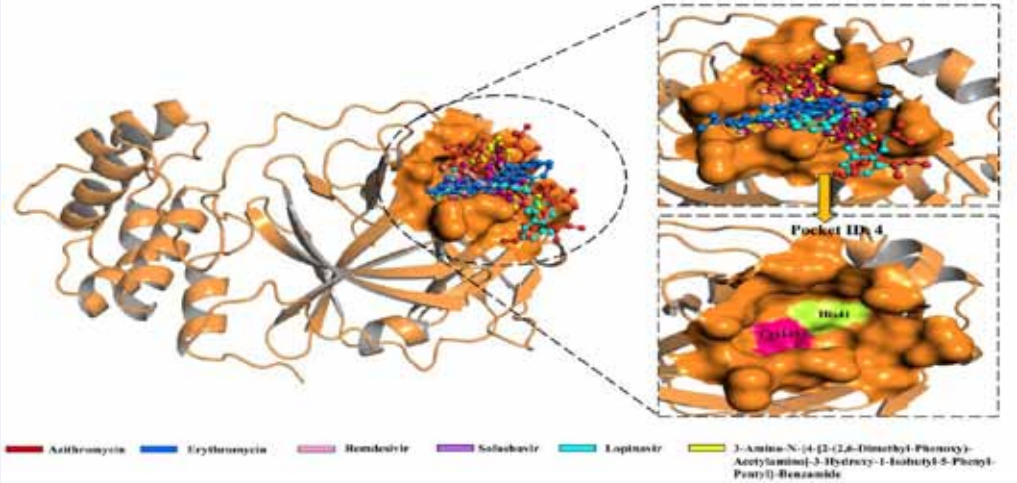

Figure 4 Biased docking in the substrate-binding pocket of the native-Mpro (PDB Id: 7NTT). Binding of six compounds (azithromycin, erythromycin, remdesivir, sofosbuvir, lopinavir and 3-Amino-N-{4-[2-(2,6-Dimethyl-Phenoxy)-Acetylamino]-3- Hydroxy-1-Isobutyl-5-Phenyl-Pentyl}-Benzamide) at the His41's ND1 position. The His41 and Cys145 in the substrate-binding pocket is forming a Cys-His catalytic dyad.

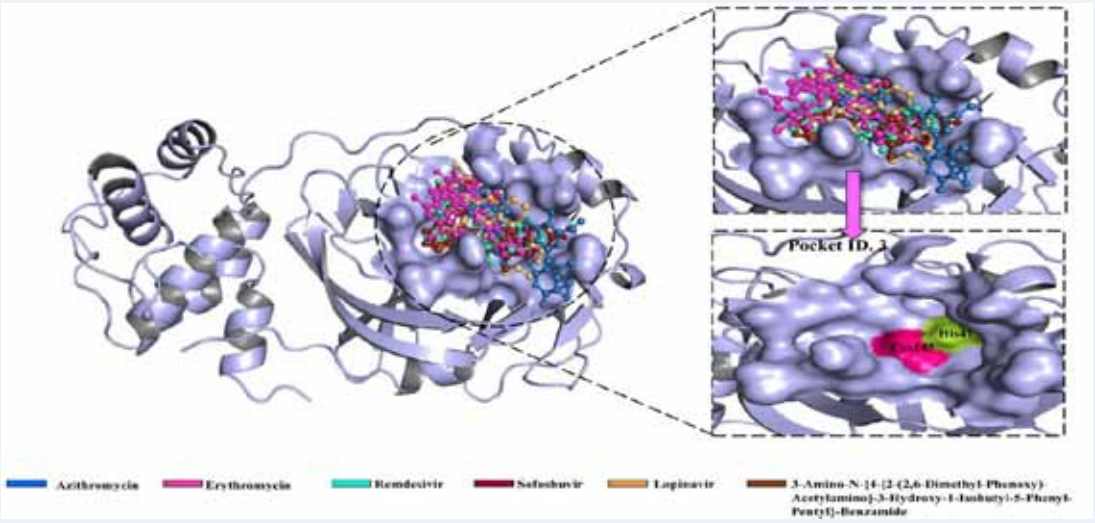

Figure 5 Biased docking in the substrate-binding pocket of the ligand-bound Mpro (PDB Id: 7VLP); Binding of six compounds (azithromycin, erythromycin, remdesivir, sofosbuvir, lopinavir and 3-Amino-N-{4-[2-(2,6-Dimethyl-Phenoxy)- Acetylamino]-3-Hydroxy-1-Isobutyl-5-Phenyl-Pentyl}-Benzamide) at the His41's NE2 position. The His41 and Cys145 in the substrate-binding pocket forming is a Cys-His catalytic dyad.

Table 1: Docking result of Native and Ligand-bound Mpro (PDB Id: 7NTT and7VLP)

Sl. No	Compound	Binding energy (Kcal/mol)		Inhibition constant, Ki (uM)		No. of H bonds (drug-enzyme)	
		Catego ry-I	Categor y-II	Catego ry-I	Categor y-II	Category-I	Category- II
1	Azithromycin	-4.52	-8.73	485.23	1.52	4	5
2	Erythromycin	-6.93	-7.26	8.37	4.76	4	8
3	Remdesivir	-7.37	-8.94	3.93	278.30	9	8
4	Sofosbuvir	-7.62	-8.94	2.61	279.66	13	6
5	Lopinavir	-7.64	-5.50	2.52	92.67	9	4
6	**3-Amino	-4.35	-8.58	647.64	517.60	7	5

** 3-Amino-N-{4-[2-(2,6-Dimethyl-Phenoxy)-Acetylamino]-3-Hydroxy-1-Isobutyl-5- Phenyl-Pentyl}-Benzamide; Category-I represents in native conformation and Category-II ligand-bound conformation.

Table 2: **Pharmacokinetics properties of azithromycin, remdesivir, and lopinavirand their structural analogues**

Drugs	cLogP	Solubility	Molecular weight	TIPSA	Drug-Likeness	Drug Score	Molar refractivity	Lipinski	Bioavailability score	Synthetic accessibility
Azithromycin	1.66	-3.09	748.99	180.08	13.85	0.52	200.78	No; 2 violations: MW>500, NorO>10	0.17	8.91
Erythromycin	1.67	-3.64	733.93	193.91	11.29	0.52	189.36	No; 2 violations: MW>500, NorO>10	0.17	8.73
Remdesivir	0.30	-4.99	602.58	213.36	-30.39	0.07	150.43	No; 2 violations: MW>500, NorO>10	0.17	6.43
Sofosbuvir	0.36	-3.78	529.46	162.54	-29.32	0.35	125.53	No; 2 violations: MW>500, NorO>10	0.17	6.12
Lopinavir	4.85	-6.13	628.81	120.00	7.64	0.27	187.92	Yes; 1 violation: MW>500	0.55	5.67
****3-Amino**	4.79	-6.13	531.69	113.68	4.10	0.32	156.51	Yes; 1 violation: MW>500	0.55	4.65

** 3-Amino-N-{4-[2-(2,6-Dimethyl-Phenoxy)-Acetylamino]-3-Hydroxy-1-Isobutyl-5-Phenyl-Pentyl}-Benzamide

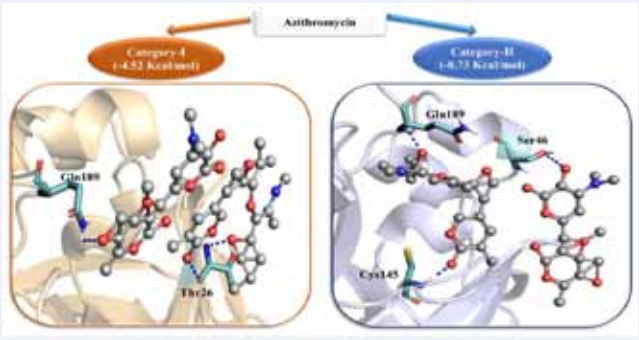

Figure 6 H-Bond interactions of the ligand (azithromycin, DB00207) with the Polar residues in the binding pocket.

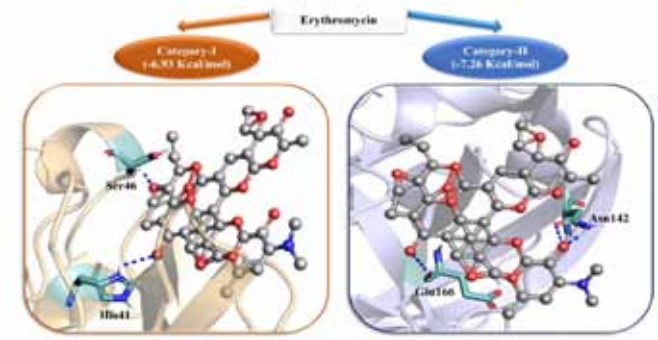

Figure 7 H-Bond interactions of the ligand (erythromycin, DB00199) with the Polar residues in the binding pocket.

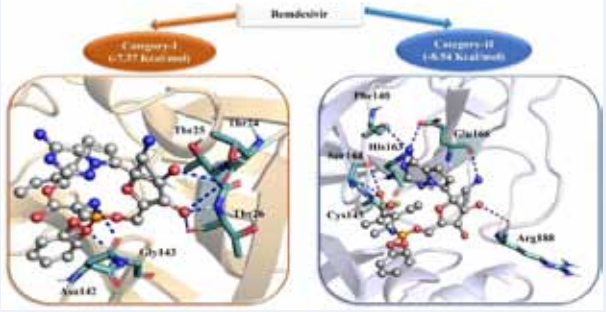

Figure 8 H-Bond interactions of the ligand (remdesivir, DB14761) with the Polar residues in the binding pocket.

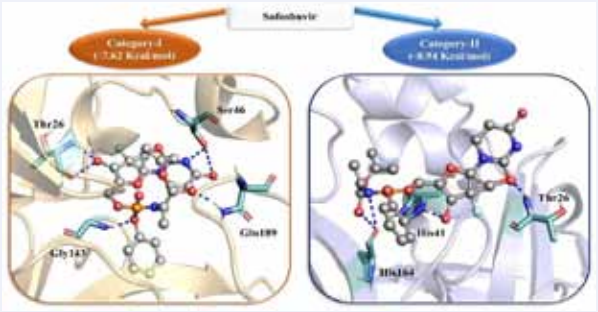

Figure 9 H-Bond interactions of the ligand (sofosbuvir, DB08934) with the Polar residues in the binding pocket.

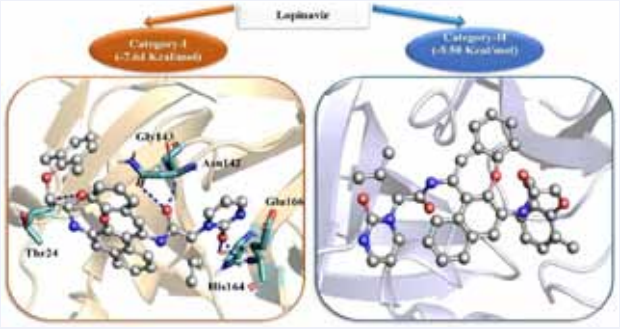

Figure 10 H-Bond interactions of the ligand (lopinavir, DB01601) with the Polar residues in the binding pocke.

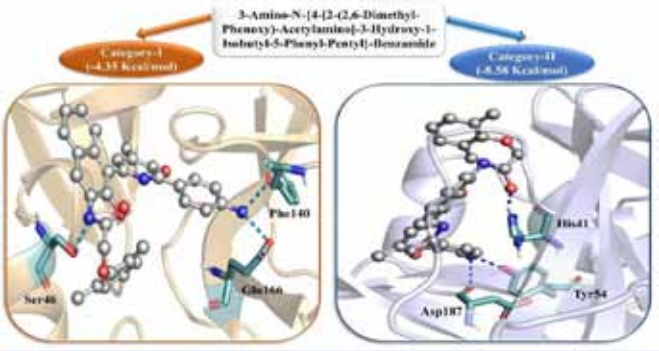

Figure 11 H-Bond interactions of the ligand (3-Amino-N-{4-[2-(2,6-Dimethyl- Phenoxy)-Acetylamino]-3-Hydroxy-1-Isobutyl-5-Phenyl-Pentyl}-Benzamide, DB04378) with the Polar residues in the binding pocket.

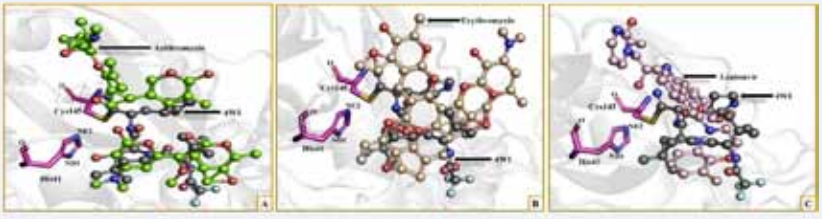

Figure 12 Superimposed complex structures between docked and the reference. ligand (4WI); (A) Superimposed complex structures of azithromycin and the reference ligand (4WI); (B) Superimposed complex structures of erythromycin and the reference ligand (4WI); (C) Superimposed complex structures of lopinavir and the reference ligand (4WI) of crystal structures suggest all the docked ligands occupy near the position of reference ligand.

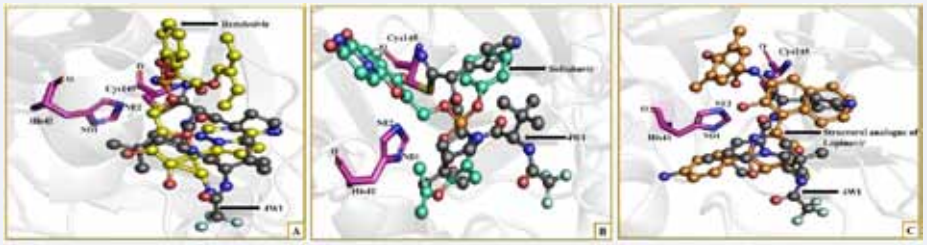

Figure 13 Superimposed complex structures between docked and the reference ligand (4WI); (A) Superimposed complex structure of remdesivir; (B) Superimposed complex structural analogues of remdesivir (sofosbuvir); (C) Superimposed complex structural analogues of lopinavir (3-Amino-N-{4-[2-(2,6-Dimethyl-Phenoxy)- Acetylamino]-3-Hydroxy-1-Isobutyl-5-Phenyl-Pentyl}-Benzamide) between docked and the reference ligand (4WI) of crystal structures suggest all the docked ligands occupy near the position of reference ligand and binds regeo-specially at NE2 position of His41 in the ligand-bound state.

To assess the statistical significance of this docking result, the physico-chemical and toxicity comparison was performed for six ligands. In the present study, OSIRIS Property Explorer was used to predict the drug-likeness score of all compounds and comparing them with the anti-biotic and antiviral drug. Moreover, the overall drug-score was estimated from summation of cLogP, solubility, TPSA, drug-likeness, drug-score, and molar refractivity parameters. Interestingly, the potential drug score of azithromycin and erythromycin are similar (0.52) but the remdesivir and lopinavir has less drug score compare to their structural analogs (Table 2).

CONCLUSION

The present study focuses on the catalytic pocket of the Mpro protein to characterize its stabilization and the role of the antibiotic and the antiviral drugs during the enzymatic mechanism. In the time of the structural transition of Mpro protein from its inactive native state to active ligand-bound form, the catalytic pocket's closing and opening mechanism may control the ligand's unbinding and binding process, which plays a decisive role in maintaining the structural architecture of this protein. How do the antibiotic azithromycin, anti-viral remdesivir, lopinavir, and their structural analogues make complex with native and ligand-bound Mpro structures, are very interesting? To answer this question, we have planned to obtain both these receptor conformations for the present investigation and thus, virtual screening with molecular docking studies has been adopted to determine the structural analogues for azithromycin, remdesivir, and lopinavir. The molecular docking between proposed drugs with native conformation of Mpro demonstrate the unrealistic binding data because the surface mouth region of catalytic pocket gets closed form, thus the drug could not able to reach at binding pocket. Hence, the findings on ligand-bound form demonstrated the following vital information that may be effective for further experimental or clinical study: (i) The antibiotic azithromycin may be used for COVID-19 disease because its structural analogue erythromycin (highly structurally similar to azithromycin and both have similar drug score) is loosely bound at the ligand-binding pocket. (ii) the anti-viral remdesivir and its analogue sofosbuvir have similar binding energy at the ligand-binding pocket of Mpro but sofosbuvir has good drug score than remdesivir, and both may be used for COVID-19. We proposed the anti- viral drug sofosbuvir may further be considered for experimental or clinical study of this disease by replacing remdesivir. (iii) another anti-viral drug, lopinavir has poor binding energy at the active conformation of catalytic pocket rather than its analogue 3-Amino-N-{4-[2-(2,6-Dimethyl-Phenoxy)-Acetylamino]-3-Hydroxy-1-Isobutyl-5-Phenyl-Pentyl}- Benzamide and also its drug score worse than its analogue. Thus the analogue of lopinavir may be used for future investigation of COVID disease. The present study should be of interest to the experimental community engaged in COVID disease and provide a testable hypothesis for future experimental and clinical validation. Our results appeared to be significant and evident that we decided to explore our essential findings with the medical community in the present pandemic situation. We, therefore, recommend that sofosbuvir is the best structural analogue for remdesivir and 3-Amino-N-{4-[2-(2,6-Dimethyl-Phenoxy)-Acetylamino]-3-Hydroxy-1-Isobutyl-5-Phenyl-Pentyl}- Benzamide of lopinavir that should be further synthesized, and require proper experimental and pre-clinical investigation for the possible treatment of nCOVID-19.

ACKNOWLEDGEMENTS

We would like to convey our special thanks to the Department of Bioinformatics, Maulana Abul kalam Azad University of Technology, W.B. for providing the computational facility and other institutional facility to conduct the research work.

REFERENCES

1. Chow EJ, Uyeki TM, Chu HY. The effects of the COVID-19 pandemic on community respiratory virus activity. Nat Rev Microbiol. 2023; 21: 195-210.
2. Alimoradi Z, Lin CY, Pakpour AH. Worldwide estimation of parental acceptance of COVID-19 vaccine for their children: a systematic review and meta-analysis. Vaccines(Basel). 2023; 11: 533.
3. WHO Coronavirus (COVID-19) Dashboard. 2023.
4. Islam F, Bibi S, Meem AF, Islam MM, Rahaman MS, Bepary S, et al. Natural bioactive molecules: an alternative approach to the treatment and control of COVID-19. Int J Mol Sci. 2021; 22: 12638.

5. Rashad A, Nafady A, Hassan MH, Mansour H, Taya U, Bazeed SE, et al. Therapeutic efficacy of macrolides in management of patients with mild COVID-19. Sci Rep. 2021; 11: 16361.

6. Hicks LA, Taylor Jr TH, Hunkler RJ. US outpatient antibiotic prescribing, 2010. N Engl J Med. 2013; 368: 1461-1462.

7. Bacharier LB, Guilbert TW, Mauger DT, Boehmer S, Beigelman A, Fitzpatrick AM, et al. Early administration of azithromycin and prevention of severe lower respiratory tract illnesses in preschool children with a history of such illnesses: a randomized clinical trial. JAMA. 2015; 314: 2034-2044.

8. Gautret P, Lagier JC, Parola P, Meddeb L, Mailhe M, Doudier B, et al. Hydroxychloroquine and azithromycin as a treatment of COVID-19: results of an open-label non-randomized clinical trial. Int J Antimicrob Agents. 2020; 56: 105949.

9. Yao X, Ye F, Zhang M, Cui C, Huang B, Niu P, et al. In vitro antiviral activity and projection of optimized dosing design of hydroxychloroquine for the treatment of severe acute respiratory syndrome coronavirus 2 (SARS-CoV-2). Clin Infect Dis. 2020; 71: 732-739.

10. Aminov RI. Biotic acts of antibiotics. Front Microbiol. 2013; 4: 241.

11. Steel HC, Theron AJ, Cockeran R, Anderson R, Feldman C. Pathogen- and host-directed anti-inflammatory activities of macrolide antibiotics. Mediators Inflamm. 2012; 2012.

12. Kumar AP, Park JH. Azithromycin as a new chiral selector in capillary electrophoresis. J Chromatogr A. 2011; 1218: 1314-7.

13. Geraghty RJ, Aliota MT. Bonnac LF. Broad-spectrum antiviral strategies and nucleoside analogues. Viruses. 2021; 13: 667.

14. Eastman RT, Roth JS, Brimacombe KR, Simeonov A, Shen M, Patnaik S, et al. Remdesivir: a review of its discovery and development leading to emergency use authorization for treatment of COVID-19. ACS Cent Sci. 2020; 6: 672-683.

15. FDA News Release. Remdesivir EUA Letter of Authorization. 2020.

16. Lopinavir, September 1, 2017.

17. Cascella M, Rajnik M, Aleem A, Dulebohn S, Di Napoli R. Features, evaluation, and treatment of coronavirus (COVID-19). StatPearls. 2023.

18. Kandeel M, Morsy MA, Abd El-Lateef HM, Marzok M, El-Beltagi HS, Al Khodair KM, et al. The Safety and Efficacy of the Protease Inhibitors Lopinavir/Ritonavir as Monotherapy or Combined with Interferon in COVID-19 Patients. Processes. 2023; 11: 398.

19. Jin Z, Du X, Xu Y, Deng Y, Liu M, Zhao Y, et al. Structure of Mpro from SARS-CoV-2 and discovery of its inhibitors. Nature. 2020; 582: 289-293.

20. Tam NM, Nam PC, Quang DT, Tung NT, Vu VV, Ngo ST. Binding of inhibitors to the monomeric and dimeric SARS-CoV-2 Mpro. RSC Adv. 2021; 11: 2926-2934.

21. Rose PW, Prlić A, Bi C, Bluhm WF, Christie CH, Dutta S, et al. The RCSB Protein Data Bank: views of structural biology for basic and applied research and education. Nucleic Acids Res. 2015; 43: D345-356.

22. Tian W, Chen C, Lei X, Zhao J, Liang J. CASTp 3.0: computed atlas of surface topography of proteins. Nucleic Acids Res. 2018; 46: W363-367.

23. Wishart DS, Feunang YD, Guo AC, Lo EJ, Marcu A, Grant JR, et al. DrugBank 5.0: a major update to the DrugBank database for 2018. Nucleic Acids Res. 2018; 46: D1074-1082.

24. Zoete V, Daina A, Bovigny C, Michielin O. Swiss. Similarity: a web tool for low to ultra high throughput ligand-based virtual screening. J. Chem. Inf. 2016; 56: 1399-1404

25. Kalra S, Chauhan A. Identification of potent COVID-19 main protease (MPRO) inhibitors from flavonoids: in silico approach: Identification of potent COVID-19 main protease (MPRO) inhibitors from flavonoids. J Ayur Holis Medi (JAHM). 2023; 11.

26. Alghamdi HA, Attique SA, Yan W, Arooj A, Albulym O, Zhu D, et al. Repurposing the inhibitors of COVID-19 key proteins through molecular docking approach. Process Biochem. 2021; 110: 216-222.

27. Gyebi GA, Ogunyemi OM, Ibrahim IM, Ogunro OB, Adegunloye AP, Afolabi SO. SARS-CoV-2 host cell entry: an in silico investigation of potential inhibitory roles of terpenoids. J Genet Eng Biotechnol. 2021; 19: 1-22.

28. Jiang X, Kumar K, Hu X, Wallqvist A, Reifman J. DOVIS 2.0: an efficient and easy to use parallel virtual screening tool based on AutoDock 4.0. Chem Cent J. 2008; 2: 1-7.

29. 29. Fuhrmann J, Rurainski A, Lenhof HP, Neumann D. A new Lamarckian genetic algorithm for flexible ligand-receptor docking. J Comput Chem2010; 31: 1911-8.

30. Yuan S, Chan HS, Hu Z. Using PyMOL as a platform for computational drug design. Wiley Interdisciplinary Reviews: Computat Mol Sci. 2017; 7: e1298.